

A General Class of Regular Black Holes based on a Smeared Mass Distribution

Alexis Larrañaga*

National Astronomical Observatory. National University of Colombia.

Alejandro Cardenas-Avendaño†

*National Astronomical Observatory. National University of Colombia and
Department of Mathematics. Konrad Lorenz University.*

Daniel Alexdy Torres‡

Department of Physics. National University of Colombia.

Abstract

We investigate the behavior of a new class of regular black holes based on a non-Gaussian smeared mass distribution. It is shown that the smeared mass distribution consideration cures the well known problems in the terminal phase of black hole evaporation. We find that there is a finite maximum temperature that the black hole reaches before cooling down to absolute zero so that the evaporation ends up in a zero temperature extremal black hole. Finally, we probe the regular characteristic of the new black holes by showing that there is no curvature singularity at the origin.

PACS: 04.70.Dy, 02.40.Gh

Keywords: physics of black holes, noncommutative geometry

*Electronic address: ealarranaga@unal.edu.co

†Electronic address: alcardenasav@unal.edu.co

‡Electronic address: daatorresba@unal.edu.co

I. INTRODUCTION

Black hole physics plays a really important role in the understanding of quantum gravity. Since Hawking found the thermal radiation emitted by a collapsing black hole using the techniques of quantum field theory in a curved spacetime background [1], extensive studies on this area have been done from several theoretical view points. However, after more than forty years of intensive research in this field, various aspects of the problem still remain unclear. In particular, a satisfactory description of the late stage of the evaporation process is still missing. One of the most interesting proposals comes from the string/black hole correspondence principle [2] which suggests that in the extreme regime of the late stage evaporation, stringy effects cannot be neglected. For example, at this stage string theory predicts that target spacetime coordinates become noncommuting operators on a D -brane [3, 4]. The idea of noncommutative spacetimes was introduced by Snyder [5] who showed that it helps to cure the divergences in relativistic quantum field theory. Recently, the interest in noncommutative spacetimes grew due to the work of Nicolini et al. in which they found a noncommutative inspired Schwarzschild black hole [6–8]. This work was extended to include the electric charge [9], extra dimensions [10, 11] and noncommutative black holes in (1+1)-dimensions [12], (2+1)-dimensions [13, 14] and in the Randall-Sundrum braneworld model [15] were also found. All these solutions share the remarkable property of the existence of an extreme mass M_0 under which no horizons are present. This fact gives as a result that there is a remnant after the Hawking evaporation finishes, which could, in principle, solve the so-called paradox of black hole information loss. In all these works, the smeared mass is mathematically introduced by replacing the point-like source with a Gaussian distribution. However, in the work of Park [16], it is pointed out that the Gaussianity is not always required and that non-Gaussian smeared mass distribution has not been studied much so far, except for (2+1) noncommutative black hole solutions found in [17] and [18]. As a deformation of the δ -function source, it is enough to require that the distribution has a sharp peak at the origin and that the integration of the distribution function gives a finite value, so that it always can be normalized to unity.

The main purpose of this paper is to obtain a new class of black hole solutions by solving Einstein equations in the presence of an anisotropic perfect fluid based on a non-Gaussian smeared mass distribution which include the Gaussian, Rayleigh, and Maxwell-Boltzmann

distributions with moments $n = 0, 1$ and 2 , respectively. The outline of this paper is as follows: in Section 2, we introduce the smeared mass distribution and the new regular black hole solution of Einstein equations. Then in Section 3, we study the thermodynamics of this noncommutative black hole to show that the evaporation process admits both a minimum and a maximum value of temperature before cooling down towards a zero temperature remnant while the final section is for the conclusions.

II. THE BLACK HOLE SOLUTION BASED ON A NON-GAUSSIAN SMEARED MASS DISTRIBUTION

The noncommutativity of spacetime can be incorporated in two ways. The first approach introduces the commutator of spacetime coordinates operators

$$[\mathbf{x}^\mu, \mathbf{x}^\nu] = i\theta^{\mu\nu}, \quad (1)$$

where $\theta^{\mu\nu}$ is a real valued anti-symmetric matrix with the dimension of length squared and which determines the fundamental cell discretization of spacetime in the same way as \hbar discretizes the phase space. Together with the Seiberg-Witten map and the Weyl-Wigner-Moyal \ast -product, this leads to correction terms in the metric.

The second approach is called the coordinate coherent state formalism [19, 20], from which the so-called noncommutative inspired black holes were obtained [6–8]. Here, the effects of noncommutativity are taken into account by keeping the usual form of the Einstein tensor in the field equations and introducing a modified energy-momentum tensor as a source [21]. Specifically, the effect of noncommutativity is incorporated by replacing the point-like mass density, described by a Dirac δ function, with a smeared object, for example a Gaussian distribution [19, 20]. However, Park [16] further pointed out that the Gaussianity is not always required and proposed a smeared source based on the Maxwell-Boltzmann mass distribution to construct a $(2 + 1)$ dimensional black hole.

Inspired by this result, we propose the mass density of a static, spherically symmetric, smeared particle-like gravitational source in the form

$$\rho(r) = Ar^n \exp\left(-\frac{r^2}{\ell^2}\right), \quad (2)$$

where ℓ is a characteristic length scale of the matter distribution and A is a normalization

constant. This density profile reproduces the Gaussian distribution of Nicolini et. al. [6] for $n = 0$ and includes non-Gaussian (i.e. ring-type) distributions for higher moments, for example Rayleigh for $n = 1$, Maxwell-Boltzmann for $n = 2$, etc. In order to obtain the constant A , we consider the mass enclosed in a volume of radius r , which must be determined by integrating the density,

$$m(r) = \int_0^r 4\pi \tilde{r}^2 \rho(\tilde{r}) d\tilde{r} = 2\pi A \ell^{n+3} \gamma\left(\frac{n+3}{2}; \frac{r^2}{\ell^2}\right), \quad (3)$$

where $\gamma\left(\frac{n+3}{2}; \frac{r^2}{\ell^2}\right)$ is the lower incomplete gamma function discussed in the Appendix. Phenomenological results imply that noncommutativity is not visible at presently accessible energies, constraining $\ell < 10^{-16} \text{cm}$ [6]. At large distances one expects minimal deviations from standard vacuum Schwarzschild geometry. In fact, the mass of the black hole M can be determined in the commutative limit $\ell \rightarrow 0$ (or equivalently $\frac{r}{\ell} \rightarrow \infty$), where the lower incomplete γ function becomes the usual gamma function, $\gamma\left(\frac{n+3}{2}; \frac{r^2}{\ell^2}\right) \rightarrow \Gamma\left(\frac{n+3}{2}\right)$, and we expect that $m(r) \rightarrow M$. This gives the normalization constant $A = \frac{M}{2\pi\Gamma\left(\frac{n+3}{2}\right)\ell^{n+3}}$ and therefore the density distribution becomes

$$\rho(r) = \frac{M}{2\pi\Gamma\left(\frac{n+3}{2}\right)\ell^{n+3}} \exp\left(-\frac{r^2}{\ell^2}\right), \quad (4)$$

which shows that the black hole mass M , instead of being perfectly localized at a single point, is diffused through a region of linear size ℓ .

Before solving the field equations we will define completely the energy-momentum tensor. In order to do it, we consider the covariant conservation condition $T^{\mu\nu}_{;\nu} = 0$ which, for a spherically symmetric metric is

$$\partial_r T^r_r = -\frac{1}{2} g^{00} \partial_r g_{00} (T^r_r - T^0_0) - g^{\theta\theta} \partial_r g_{\theta\theta} (T^r_r - T^\theta_\theta). \quad (5)$$

We want to preserve the Schwarzschild-like property $g_{00} = -g_{rr}^{-1}$, so we require $T^r_r = -T^0_0 = \rho(r)$. Therefore, the divergence free equation allows a solution for T^θ_θ which reads

$$T^\theta_\theta = -\rho(r) - \frac{r}{2} \partial_r \rho(r). \quad (6)$$

Note that, rather than a massive structureless point, the proposed source turns out to be a self-gravitating, droplet of anisotropic fluid of density ρ , radial pressure $p_r = -\rho$ and tangential pressure

$$p_{\perp} = -\rho - \frac{r}{2}\partial_r\rho(r). \quad (7)$$

These equations turn out to mean that, on physical grounds, there is a non-vanishing radial pressure balancing the inward gravitational pull and thus, preventing the collapse of the droplet into a matter point. This is precisely the physical effect on matter caused by spacetime noncommutativity and the origin of all new physics at short distance scales.

In order to obtain a black hole solution, we solve the Einstein equations

$$G_{\nu}^{\mu} = R_{\nu}^{\mu} - \frac{1}{2}g_{\nu}^{\mu}R = 8\pi T_{\nu}^{\mu} \quad (8)$$

with (4) as the matter source and using the line element

$$ds^2 = f(r)dt^2 - \frac{dr^2}{f(r)} - r^2(d\theta^2 + \sin^2\theta d\phi^2). \quad (9)$$

This gives the function

$$f(r) = 1 - \frac{M}{4\pi r\Gamma\left(\frac{n+3}{2}\right)}\gamma\left(\frac{n+3}{2}, \frac{r^2}{\ell^2}\right), \quad (10)$$

which is the same result obtained by simply substituting the mass function (3) into the mass term of Schwarzschild metric. Therefore the classical Schwarzschild metric is obtained from this solution in the limit $\frac{r}{\ell} \rightarrow \infty$.

The line element (9) describes a regular black hole and should give us useful insights about possible spacetime noncommutativity effects on Hawking radiation. Possible horizon(s) of this solution can be obtained by solving the equation $f(r) = 0$, that is

$$r_H = \frac{M}{4\pi\Gamma\left(\frac{n+3}{2}\right)}\gamma\left(\frac{n+3}{2}, \frac{r_H^2}{\ell^2}\right). \quad (11)$$

This equation cannot be solved for r_H in a closed form, but, by plotting $f(r)$ one can determine numerically the existence of horizon(s) and their radius by reading the intersections with the r -axis. From Figure (1) is easy to note that the smeared mass distribution introduces new behavior with respect to Schwarzschild black hole. In fact, instead of a single event horizon, for each value of n in $f(r)$, there are three different possibilities:

1. two distinct horizons for $M > M_0$
2. one degenerate horizon in r_0 , corresponding to an extremal black hole

3. no horizon for $M < M_0$.

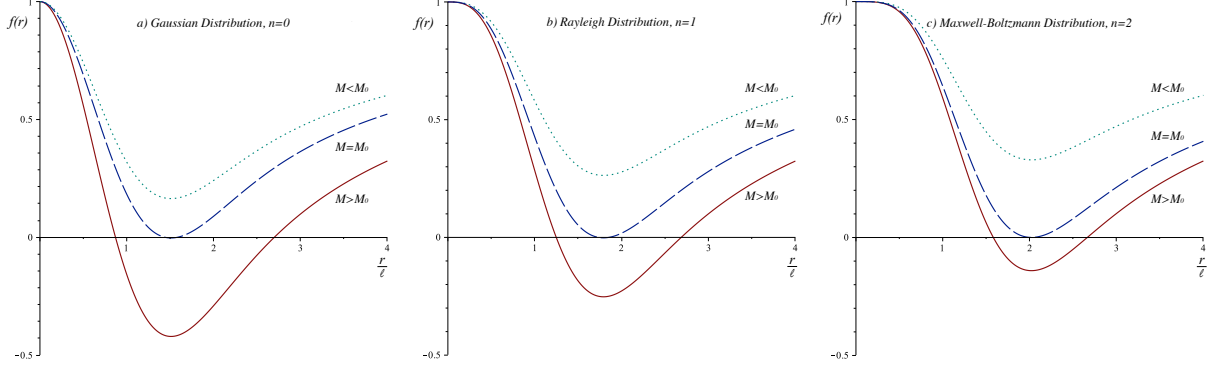


Figure 1: $f(r)$ vs $\frac{r}{\ell}$, for various values of n . Intercepts on the horizontal axis give radii of the event horizons. Figure a) shows the Gaussian distribution, $n = 0$, figure b) corresponds to the Rayleigh distribution, $n = 1$ and figure c) is the Maxwell-Boltzmann distribution, $n = 2$. In all cases the red continuous line represents a black hole with two horizons, $M > M_0$, the dashed blue line corresponds to the extreme black hole with one degenerate horizon, $M = M_0$, and the dotted green line shows a solution with no horizons $M < M_0$. The specific value of M_0 depends on the value of the length ℓ and on the exponent n .

Therefore, we conclude that there is no black hole if the original mass is less than the minimal mass M_0 which depends on the value of the length ℓ and on the exponent n . Furthermore, contrary to the usual Schwarzschild black hole, there can be two horizons for large masses. It also can be seen that for $M \gg M_0$, the inner horizon shrinks to zero while the outer one approaches the Schwarzschild horizon, located at $r_S = 2M$.

III. THERMODYNAMICS

The temperature associated with the black hole is given by

$$T = \left(\frac{1}{4\pi} \frac{df}{dr} \right)_{r=r_H} = \frac{1}{4\pi r_H} \left[1 - 2 \frac{r_H^{n+3}}{\ell^{n+3}} \frac{e^{-\frac{r_H^2}{\ell^2}}}{\gamma\left(\frac{n+3}{2}, \frac{r_H^2}{\ell^2}\right)} \right], \quad (12)$$

where we have used the derivative of the lower incomplete gamma function described in the Appendix and equation (11) to write M in terms of r_H . It is clear that the second term inside the brackets is the correction arising from the smeared distribution. For large black holes, i.e. $\frac{r_H^2}{\ell^2} \gg 1$, equation (12) recovers the standard Hawking temperature for the Schwarzschild black hole,

$$T_H = \frac{1}{4\pi r_H} . \quad (13)$$

In Figure (2) we plot the temperature (12) as a function of r_H and we find that at the initial state of evaporation the black hole temperature increases while the horizon radius is decreasing. Here, the interesting point is to investigate what happens as we reach the final state of the process, i.e. when $r_H \rightarrow \ell$. As is well known, in the standard case the Hawking temperature T_H diverges as $M \rightarrow 0$, or equivalently $r_H \rightarrow 0$. However, in our solution the temperature (12) deviates from the standard hyperbola (13) and instead of exploding, it reaches a maximum value and then it quickly drops to zero for $r_H = r_0$, leaving a frozen extremal black hole. In the region $r_H < r_0$ there is no black hole, because physically T cannot be negative. As is easily observed, the Hawking paradox is circumvented by the smeared mass distribution.

IV. CURVATURE SCALARS

We approach the regularity problem of the solution by studying the behavior of two curvature scalars, the Ricci scalar $R = g^{\mu\nu} R_{\mu\nu}$ with $R_{\mu\nu}$ the Ricci tensor, and the Kretschmann invariant $K = R_{\mu\nu\rho\sigma} R^{\mu\nu\rho\sigma}$ with $R_{\mu\nu\rho\sigma}$ the Riemann tensor. For our black hole solution, these invariants are

$$R = \frac{M}{2\pi\Gamma\left(\frac{n+3}{2}\right)} \frac{r^n}{\ell^{n+3}} e^{-\frac{r^2}{\ell^2}} \left[2\frac{r^2}{\ell^2} - (n+4) \right] \quad (14)$$

and

$$K = \left(\frac{M}{2\pi\Gamma\left(\frac{n+3}{2}\right)} \right)^2 \times \left\{ \frac{3}{r^6} \gamma^2 \left(\frac{n+3}{2}, \frac{r_H^2}{\ell^2} \right) + 2\gamma \left(\frac{n+3}{2}, \frac{r_H^2}{\ell^2} \right) \left[(n-2) - 2\frac{r^8}{\ell^2} \right] \frac{r^{n-3}}{\ell^{n+3}} e^{-\frac{r^2}{\ell^2}} + \left[n^2 + 4 - 4n\frac{r^2}{\ell^2} + 4\frac{r^4}{\ell^4} \right] \frac{r^{2n}}{\ell^{2n+6}} e^{-2\frac{r^2}{\ell^2}} \right\} \quad (15)$$

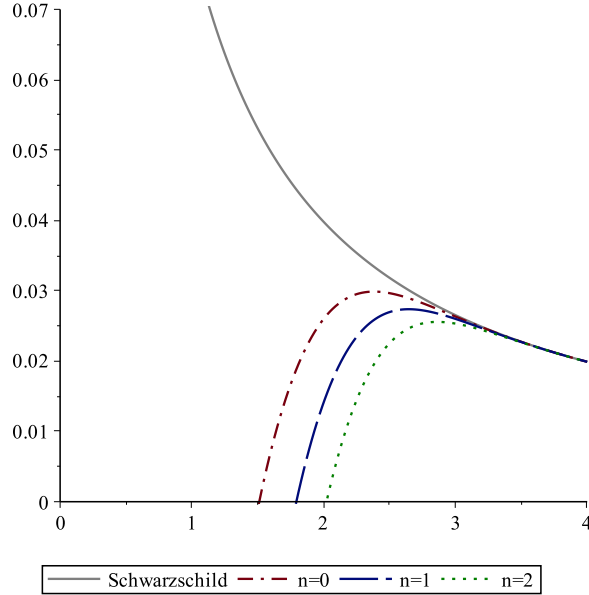


Figure 2: Plot of T vs $\frac{r_H}{\ell}$, for different values of n . Intercepts on the horizontal axis give radii of the event horizon of the extremal black hole. $n = 0$, (Gaussian distribution, dot-dashed red curve), $n = 1$, (Rayleigh distribution, dashed blue curve) and $n = 2$ (Maxwell-Boltzmann distribution, dotted green curve). For comparison, we also plotted in black the standard Hawking temperature of Schwarzschild black hole. The temperatures coincide for $\frac{r_H}{\ell} \gg 1$.

For $M \neq 0$, these invariants are regular everywhere, including the point $r = 0$. In fact, both invariants vanish at the origin for all values of n except in the case $n = 0$, for which the invariants take a constant value (see Figure 3).

V. CONCLUSION

We have shown that the introduction of smeared mass distributions in general relativity as the matter source, inspired by the noncommutativity of spacetime, gives a general class of regular black holes that reproduces, as special cases, the Gaussian distribution of Nicolini et. al. [6] for $n = 0$ and includes non-Gaussian (i.e. ring-type) distributions for higher moments,

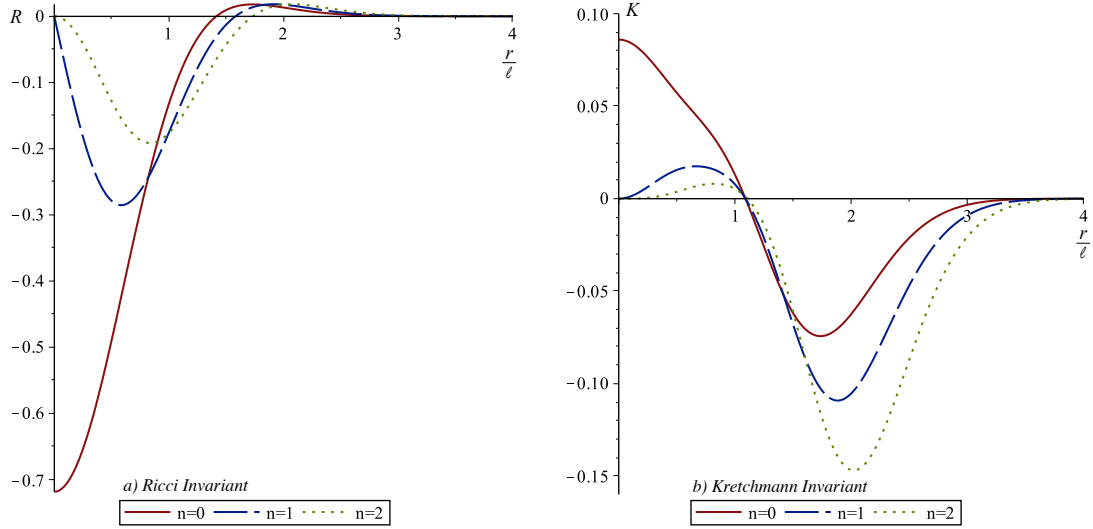


Figure 3: a) Plot of the Ricci invariant R as function of the radial coordinate $\frac{r}{\ell}$. b) Plot of the Kretschmann invariant K as function of the radial coordinate $\frac{r}{\ell}$. The graphics show the behavior of the invariants near $r = 0$ for different values of n . In both figures the Gaussian distribution $n = 0$, is the continuous red curve, the Rayleigh distribution $n = 1$, is dashed blue curve and the Maxwell-Boltzmann distribution $n = 2$, corresponds to the dotted green curve.

for example Rayleigh for $n = 1$, Maxwell-Boltzmann for $n = 2$, etc. The energy-momentum tensor needed for this description is that of an ideal fluid and requires a non-trivial pressure.

We also investigate the temperature of our regular black holes based on a smeared mass distribution to show that there is a maximum value that the black hole can reach before cooling down to absolute zero corresponding to an extreme black hole remnant. The size of this remnant depends on the value of the minimal length ℓ and on the value of the exponent n in the mass distribution. Therefore, we conclude that the smeared source regularizes divergent quantities in the final stage of black hole evaporation (in the same way that the noncommutativity approach regularizes UV infinities in quantum field theory).

Finally we study the behavior of two curvature invariants and the everywhere regular geometry, together with the existence of the residual mass M_0 , are both manifestations of the de-localization of the source. The same kind of regularization is the one that eliminates

the divergent behavior of temperature associated with the black hole.

Acknowledgement

This work was supported by the Universidad Nacional de Colombia. Hermes Project Code 18140.

Appendix

The lower incomplete gamma function $\gamma(a, x)$ is given by

$$\gamma(a, x) \equiv \int_0^x t^{a-1} e^{-t} dt \quad (16)$$

while the upper incomplete gamma function $\Gamma(a, x)$ is

$$\Gamma(a, x) \equiv \int_x^\infty t^{a-1} e^{-t} dt \quad (17)$$

and their sum corresponds to the total gamma function

$$\Gamma(a) = \gamma(a, x) + \Gamma(a, x) = \int_0^\infty t^{a-1} e^{-t} dt. \quad (18)$$

The derivative of the lower incomplete gamma function is

$$\frac{\partial}{\partial x} \gamma(a, x) = e^{-x} x^{a-1}. \quad (19)$$

-
- [1] S. W. Hawking, Comm. Math. Phys. **43**, 199 (1975).
 - [2] L. Susskind, Phys. Rev. Lett. **71**, 2367 (1993).
 - [3] E. Witten, Nucl. Phys. B **460**, 335 (1996).
 - [4] N. Seiberg, E. Witten, JHEP **9909**, 032 (1999).
 - [5] H. S. Snyder, Phys. Rev. **71** 38 (1947).
 - [6] Nicolini P, Smailagic A, Spallucci E. Phys. Lett. B, **632**, 547 (2006).
 - [7] Nicolini P, Smailagic A, Spallucci E. ESA Spec. Publ. **637**, 111 (2006).
 - [8] Nicolini P. J. Phys. A **38**, L631 (2005).
 - [9] Ansoldi S et al. Phys. Lett. B **645**, 261 (2007).

- [10] Rizzo T G. J. High Energy Phys. **0609**, 021 (2006).
- [11] Spallucci E, Nicolini P, Smailagic A. Phys. Lett. B **670**, 449 (2009).
- [12] Mureika J R, Nicolini P. Phys. Rev. D **84**, 044020 (2011).
- [13] Myung Y S, Kim Y W, Park Y. J. High Energy Phys. **0702**, 012 (2007).
- [14] Tejeiro J M, Larranage A. Pramana J. Phys. **78**, 1 (2012).
- [15] A. Larrañaga, C. Benvides and C. Rodriguez. Rom. J. Phys. **59**, 57 (2014).
- [16] Park M I. Phys. Rev. D **80**, 084026 (2009).
- [17] Myung Y S, Yoon M. Eur. Phys. J. C **62**, 405 (2009).
- [18] Liang, J., Liu Y. C., Zhu Q. Chinese Physics C **38**, 2, 025101 (2014).
- [19] A. Smailagic, E. Spallucci, J. Phys. A **36**, L467 (2003).
- [20] A. Smailagic, E. Spallucci, J. Phys. A **36** L517 (2003).
- [21] Nicolini P. Int. J. Mod. Phys. A **24**, 1229 (2009).